NONDESTRUCTIVE CHARACTERIZATION OF THE ELASTIC PROPERTIES OF ORTHOTROPIC COMPOSITES WITH ULTRASOUND

MATHIAS KERSEMANS[1*], WIM VAN PAEPEGEM[1], FILIP ZASTAVNIK[2], JUN GU[2], HUGO SOL[2] AND JORIS DEGRIECK[1]

[1] Department of Materials Science and Engineering, Ghent University, Technology park 903, 9052 Zwijnaarde, Belgium
[2] Department Mechanics of Materials and Constructions, Free University of Brussels, Pleinlaan 2, 1050 Brussels, Belgium
[*]Email address: Mathias.Kersemans@UGent.be

I. INTRODUCTION

Due to the increasing use of composite materials in critical applications demanding light weight to high strength ratio, reliable evaluation tools are necessary. The field of ultrasound is a well known non-destructive method, in which the classical C-scan has already proven its usefulness in visualizing defects, delaminations, ... (ref. 1, 2, 3). Though, one of the most critical degradation mechanisms involves fatigue of composite materials, which is attended with a local reduction of the stiffness of the material . Because of the inherent limitations of a C-scan for quantitative characterization (ref. 1) , more sophisticated non-destructive tools are needed to monitor complex damage mechanisms.
By gathering the reflected (or transmitted) amplitude of a bounded ultrasonic beam, impinging from every possible angle of incidence, one is able to build a polar plot covering a certain solid angle (ref. 4, 5, 6). This is schematically shown in figure 1, the radius of a polar plot corresponding to θ, the polar angle to φ. Typically, dark rings are observed in a polar plot which can be linked to the generation of critical bulk waves (pulsed regime) or to the generation of guided waves (harmonic regime). Both types of waves are vigorously entangled with the elastic constants of the material, thus a local fingerprint of the material under investigation is gathered (ref. 7, 8, 9).
A short introduction of the physical background, of the polar scan, is given in the next section. The in-house developed experimental test setup is presented in the third section. Finally, we show some experimental and numerical results for orthotropic carbon fabric/PPS laminate as well as unidirectional (UD) carbon/epoxy, using both pulsed and harmonic ultrasonic beams. The results are discussed in order to get an understanding of the observed complex patterns.

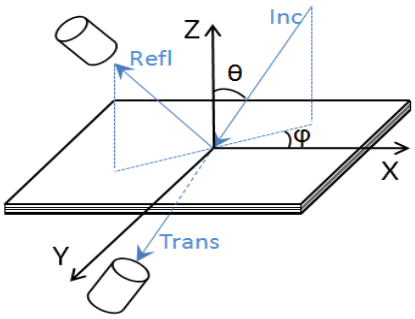

Figure 1: Schematic of the principle of the polar scan, together with the definition of the most important coordinates.

II. PHYSICAL BACKGROUND OF POLAR SCAN

In general, an unbounded material possesses three distinct bulk waves, one (quasi-) longitudinally and two (quasi-) transversally polarized ones. Each of them having a characteristic phase velocity c_{ph} (analogously a characteristic wave vector $\boldsymbol{k}$), which is determined by the physical properties, more precise the elasticity constants C_{ij} and density ρ, of the material under investigation (ref. 8). To promote the transfer of acoustical energy in the solid layer, a coupling medium, e.g water, is often used. Snell-Descartes' law which states that $k_1=k_1^{liq}$ and $k_2=k_2^{liq}$, for interfaces perpendicular to k_3, must be taken into account for external borne (denoted with superscript 'liq') sound propagating in a material. This leads to the concept of critical angles, at which the impinging wave is refracted with its wave vector $\boldsymbol{k}$ parallel to the interface. A sharp discontinuity is observed in the reflection (transmission) curves, leading to the characteristic patterns of a polar plot. The critical bulk angles, computed for some typical composite materials immersed in water, are presented in polar form in Figure 2.

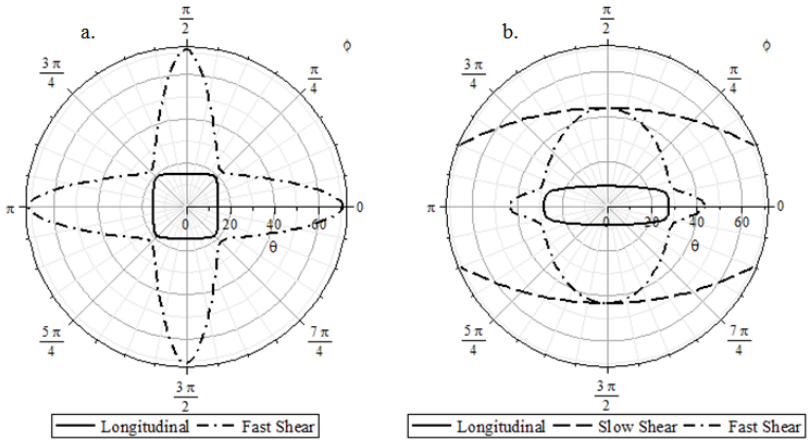

Figure 2: Critical bulk angles for (a) carbon fabric/PPS laminate and (b) Unidirectional carbon/epoxy. The anisotropic nature of the materials clearly being reflected in the curves.

The calculations for the orthotropic carbon fabric/PPS laminate are performed using the material parameters given in (ref. 10, Table 4, PBC and Volume averaging), while the constants for UD carbon/epoxy are determined within our research team. Both set of parameters are listed in Table 1.

Table 1: Material constants of UD carbon/epoxy (65%-35% proportion) and carbon fabric/PPS laminate used for computations.

	E_{11} [GPa]	E_{22} [GPa]	E_{33} [GPa]	ν_{12}	ν_{13}	ν_{23}	G_{12} [MPa]	G_{13} [MPa]	G_{23} [MPa]	ρ [Kg/m^3]
UD	154.13	14.79	14.79	0.17	0.17	0.30	7480	7480	3370	1614
fabric	56.49	56.41	10.53	0.08	0.41	0.41	4280	3048	3045	1750

One notices the (partial) absence of the slow shear wave in Figure 2, which is simply caused by the fact that its associated phase velocity c_{ph} is smaller than the longitudinal phase velocity of water. According to Snell-Descartes' law, this would lead to an imaginary refractive angle, which has, for the present application, no physical meaning.

In reality, structural materials are bounded in space, resulting into the possible generation of so called (quasi-) Lamb waves (ref. 11, 12). These waves propagate along the plate structure, with a standing wave pattern through the thickness of the layer. Because they are physically guided by the plate, one often terms them as 'guided modes'. Mathematically, the guided modes are understood as a linear combination of the bulk waves, having a resultant wave vector $\boldsymbol{k}$ along the interface (ref. 9). Contrary to the case of bulk waves, the number of possible Lamb modes is not limited to a fixed number. Acoustical frequency f and thickness d of the material largely prescribe the number of Lamb modes, while the material parameters (C_{ij} and ρ) define their exact conditions of existence, i.e. the needed incident angle to efficiently generate them. Similar to the case of bulk waves, the generation of a Lamb mode results in a peak (valley) in the topology of the reflection (transmission) coefficient. For completeness, it is mentioned that material damping (which can be effectively modeled by considering an imaginary elasticity tensor), does not affect the position of the pattern, but rather the amplitude of the polar plot. In Figure 3, one observes several curves, prescribing the existence conditions of Lamb waves for a carbon fabric/PPS laminate in different φ-directions. The frequency-thickness product fd is put on the x-axis, while the y-axis is characterized by the incident angle θ. Because of their highly dispersive nature, these curves are termed dispersion curves. Note the addition of the bulk solutions in Figure 3 (indicated with arrows), which are recognized by their non-dispersive course. The orthotropic nature of the considered material, introduces the dependency of polar angle φ on the generation of Lamb waves. Along the symmetry axes, the term 'quasi', which is a consequence of the anisotropic material properties, can be omitted, thus resulting in 'pure' modes.

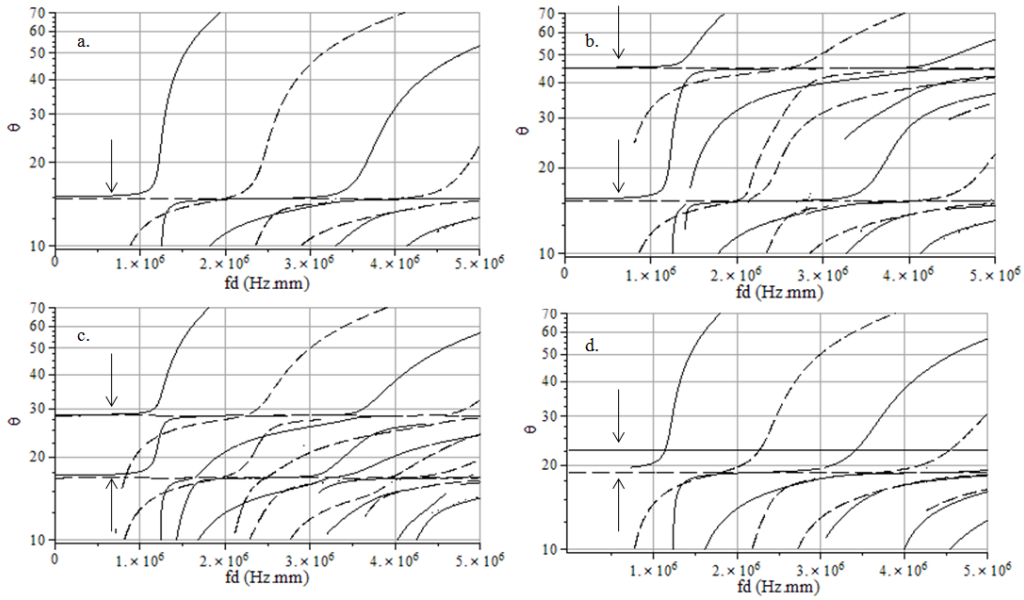

Figure 3: Dispersion curves θ(fd) for an immersed carbon fabric/PPS laminate for several polar angles: φ = 0° (a), φ = 15° (b), φ = 30° (c) and φ = 45° (d).

In practice, one can use a pulsed or harmonic incident ultrasonic beam. It is observed that a pulsed beam (typical values for *fd* are in the range of 2-10 MHz.mm) produces a fingerprint which converges to the patterns associated with the bulk solutions. This can be understood in terms of the highly dispersive character of the Lamb modes, together with its overall behavior (ref. 8). Though, for the present report, the exact deeper physical meaning is of no interest. An incoming harmonic beam on the other hand, produces the conditions to efficiently excite a Lamb mode.

III. EXPERIMENTAL SETUP

To perform the measurements with good accuracy, an in-house developed robot is constructed (Figure 4b). The setup consists of 5 axes of freedom, which allows the operator to perform both a C-scan and a polar scan of the material under investigation. The steering of the axes are programmed using LABVIEW in order to describe part of a spherical surface with its center point located at the zone under investigation. Position feedback is assured by linear resp. rotary encoders with an accuracy of 0.007 mm resp. 0.1°.
The machine can be operated in both the pulsed regime, using the OMNISCAN pulse generator (center frequency of 1 - 5 Mhz), and the harmonic regime, using the GYMNA 330 apparatus operating at *f* = 1Mhz. The coupling medium is water, enhancing the energy transfer into the solid layer. The measurements in this report are gathered in transmission, although it is straightforward to receive them in reflection. Using an acoustic mirror at the backside, one is able to operate in the double-transmission regime, which shows considerably more details because the acoustic wave undergoes two times the influence of the material. However practical considerations prevent this technique to be employed in future industrial applications and thus is not further investigated. We used the Gen5i-oscilloscope as well as the USIP20 to process the large amount of data. In order to further reduce the experimental time, the symmetry of the material can be exploited.

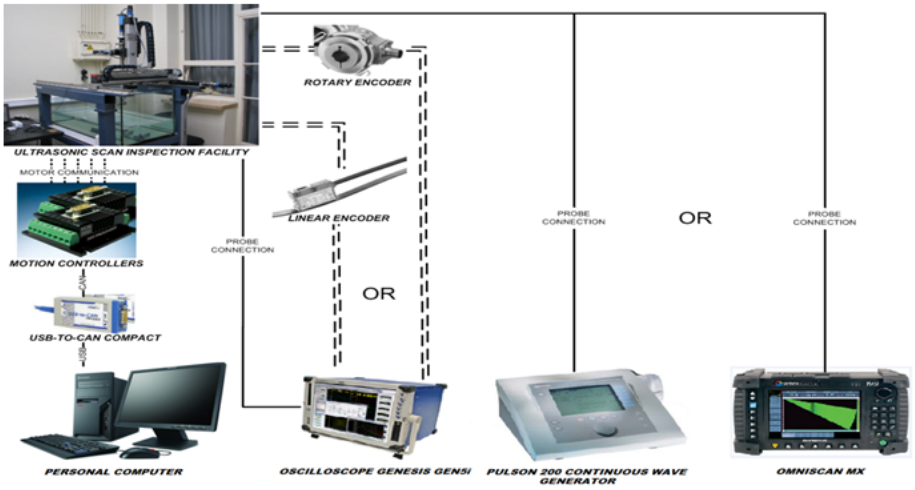

Figure 4: Experimental setup in which the GEN5i is used for data-acquisition.

IV. RESULTS AND DISCUSSION

Figure 5 shows numerically computed polar scans in transmission for the carbon fabric/PPS laminate (thickness d = 2 mm) for several operating frequencies. Comparison of the computed polar plots and the dispersion curves (Figure 5, resp. Figure 3), clearly shows the link between the observed dark regions and the generation of Lamb modes. For high fd-values, the Lamb solutions converge towards the bulk solutions, causing the dark regions being pushed outwards to the bulk solutions (Figure 2a).

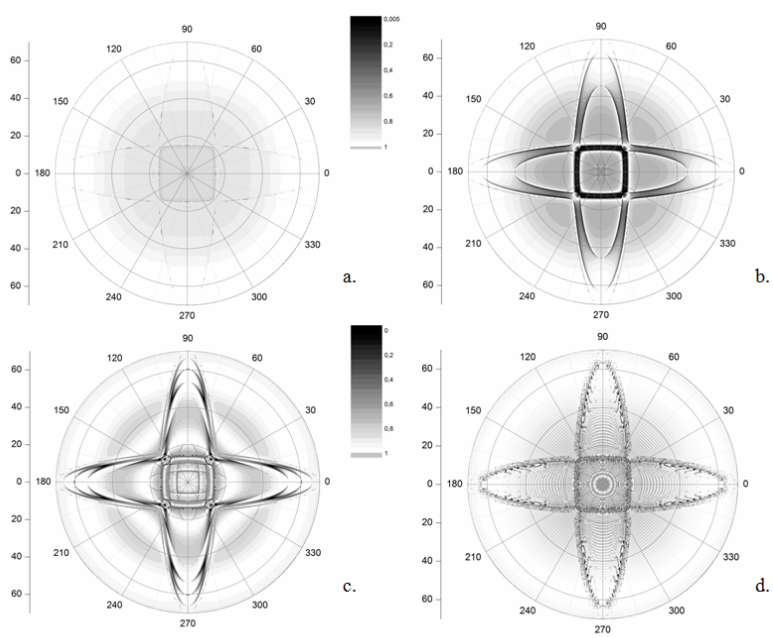

Figure 5: Numerically computed polar scan (normalized) of an immersed carbon fabric/PPS laminate, with thickness d =2 mm, using an incident harmonic beam: fd = 0.2 MHz.mm (a), f = 2 MHz.mm (b), f = 5 MHz.mm (c) and f = 25 MHz.mm (d).

Some preliminary experiments of the carbon fabric/PPS laminate are performed using an harmonic ultrasonic beam with frequency f = 1 Mhz (see Figure 6). The assumption that the carbon fabric/PPS laminate behaves as an orthotropic material, is roughly reflected in the observed experimental fingerprints for both samples. The

experimental data of sample 1 (thickness $d \approx 2$ mm) shows some peculiarities (Figure 6a):

1. the shape of the 'arms' is slightly different for various polar angles
2. the intensity of the 'arms' is slightly different for various polar angles.

Close inspection of the 'arms' reveals the appearance of two dark contours (indicated with arrows for one arm), similar as seen in the numerically computed polar plot in Figure 5b. For the second sample (Figure 6b), one observes darker and broadened contours of the narrowed 'arms'. Furthermore, a contour is observed which seems to be quasi-circular, thus reflecting isotropic behavior, at $\theta = 40°$ (indicated with an arrow). Figure 5c shows a similar sort of pattern in the numerically calculated plot. Indeed, for a vertically polarized shear wave, the plane containing the depth axis, can be regarded as an isotropic plane for the mentioned material. The inner square of the polar plot of sample 2 is largely unaltered compared to the one of sample 1, which is easily understood using the dispersion curves (Figure 3).

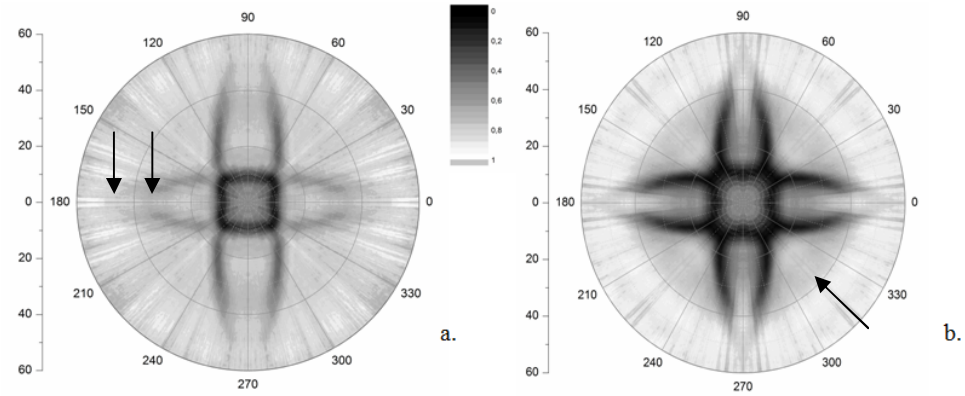

Figure 6: Experimentally registered polar scan (normalized) of an immersed carbon fabric/PPS laminate, using an incident harmonic beam of 1 MHz: fd = 2 MHz.mm (a) and fd = 6 MHz.mm (b). Some indicators are added for clarity.

Figure 7 shows some results for UD carbon/epoxy with thickness $d \approx 2$ mm using a pulsed beam with center frequency $f = 1$ MHz, thus resulting in a value of $fd = 2$ MHz.mm. One unambiguously recognizes the experimental fingerprint with the numerical results, although it is rigidly rotated over ~ 23° (the symmetry plane of the sample was not aligned with the starting scan direction). The degeneracy of the two shear bulk waves, introduced by the equivalence of the 12-direction and the 13-direction, is clearly seen.

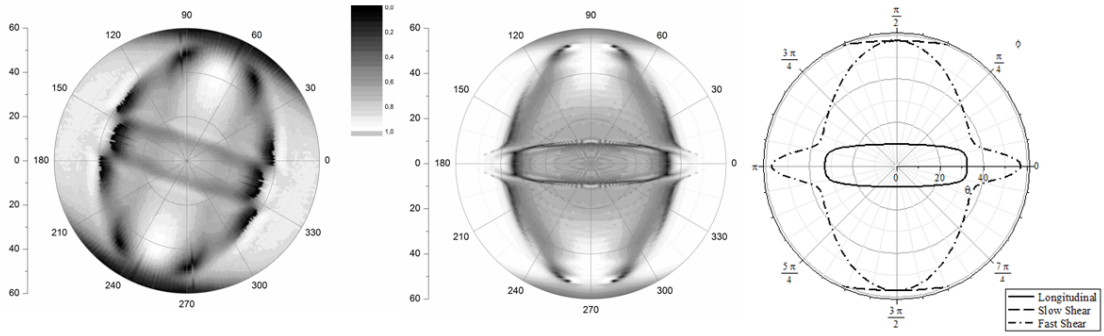

Figure 7: Experimentally registered polar scan of UD carbon/epoxy with thickness d = 2 mm, for a pulsed ultrasonic beam with center frequency f = 1 MHz (a), numerically calculated polar scan for a typical ultrasonic puls with center frequency f = 1 MHz (b) and numerically computed critical bulk angles (c).

The presented results show some deviations concerning the exact position of the observed dark regions. Possibly, slightly different material parameters are taken into account to compute the numerical results. In a next step, the physical material parameters will be optimized in order to reconstruct the experimental fingerprint and hence obtain the exact material parameters.

V. CONCLUSION

We presented numerical and experimental polar scans, using harmonic and pulsed ultrasound, for two typical anisotropic materials immersed in water. Several interesting phenomena are recognized, linking the mapped amplitude to the internal stiffness of the investigated material. There is good agreement between the experiments and theory. In the future the experimental setup will be refined, in order to enhance the resolution and to lower the experimental time. Emphasis will be put in the inverse modeling to retrieve the exact material constants. Currently, damaged materials are experimentally investigated in order to examine the influence of fatigue, delamination, etc. on the fingerprint. Premature results already indicate severe changes in the polar plot.
The fact that the reported method is

1. easy to implement in industrial applications
2. gathers information locally
3. can be simulated relatively easy
4. works in reflection

makes it an interesting candidate in the field of quantitative non-destructive testing of complex structural components.

REFERENCES

[1] A.M. I. Amenabar, A. López-Arraiza, M. Lizaranzu, J. Aurrekoetxea, Comparison and analysis of non-destructive testing techniques suitable for delamination inspection in wind turbine blades, Composites Part B: Engineering 42 (2011).
[2] Y.J. Dong, N. Ye, Y.L. Bai, On-line observation of interlaminar damage by ultrasonic inspection. Composites Science and Technology 59 (1999) 957-961.
[3] S.C. Wooh, C. Wei, A high-fidelity ultrasonic pulse-echo scheme for detecting delaminations in composite laminates. Composites Part B-Engineering 30 (1999) 433-441.
[4] N.F. Declercq, J. Degrieck, O. Leroy, Simulations of harmonic and pulsed ultrasonic polar scans. Ndt & E International 39 (2006) 205-216.
[5] W.H.M. Vandreumel, J.L. Speijer, non-destructive composite laminate characterization by means of ultrasonic polar-scan. Materials Evaluation 39 (1981) 922-925.
[6] N.F. Declercq, J. Degrieck, O. Leroy, Ultrasonic polar scans: Numerical simulation on generally anisotropic media. Ultrasonics 45 (2006) 32-39.
[7] A.H. Nayfeh, D.E. Chimenti, Ultrasonic wave reflection from liquid-coupled orthotropic plates with application to fibrous composites. Journal of Applied Mechanics-Transactions of the Asme 55 (1988) 863-870.
[8] J.L. Rose, Ultrasonic Waves in Solid Media, Cambridge University Press, 1999.
[9] B.A. Auld, Acoustic Fields and Waves in Solids, second edition, 1990.

[10] S. Daggumati, W. Van Paepegem, J. Degrieck, J. Xu, S.V. Lomov, I. Verpoest, Local damage in a 5-harness satin weave composite under static tension: Part II - Meso-FE modelling. Composites Science and Technology 70 (2010) 1934-1941.
[11] I.A.Viktorov, Rayleigh and Lamb waves, Plenum, New York, 1967.
[12] H. Lamb, On waves in an elastic plate. Proc. R. Soc. London Ser. A93 (1917).